

# Copper Mineralization in the Lower Cambrian Cover of Jbel N'Zourk (Central Anti Atlas, Morocco): Tectonic-Mineralizations Relationships

Achraf Ait Yazza<sup>1</sup>, Ismail Bouskri<sup>2</sup>, Mohamed Raji<sup>1</sup>, Faouziya Haissen<sup>1</sup>, Noura Zoraa<sup>1</sup>

<sup>1</sup>LGAGE, Faculty of Sciences Ben M'Sik, Hassan II University, Casablanca, Morocco

<sup>2</sup>SOMIFER, Managem Group/Al Mada, Casablanca, Morocco

Email: achraf.aityazza-etu@etu.univh2c.ma

**How to cite this paper:** Ait Yazza, A., Bouskri, I., Raji, M., Haissen, F. and Zoraa, N. (2023) Copper Mineralization in the Lower Cambrian Cover of Jbel N'Zourk (Central Anti Atlas, Morocco): Tectonic-Mineralizations Relationships. *Open Journal of Geology*, **13**, 1195-1219.

<https://doi.org/10.4236/ojg.2023.1311051>

**Received:** August 24, 2023

**Accepted:** November 19, 2023

**Published:** November 22, 2023

Copyright © 2023 by author(s) and Scientific Research Publishing Inc. This work is licensed under the Creative Commons Attribution International License (CC BY 4.0).

<http://creativecommons.org/licenses/by/4.0/>



Open Access

## Abstract

The Moroccan Anti-Atlas is a vast geological region composed of a Precambrian basement covered by a late-Neoproterozoic to Paleozoic sedimentary sequences. More than 200 copper occurrences are listed in these sequences. The copper mineralization of the Jbel N'Zourk (Central Anti-Atlas) is observed into the lower Limestones of the lower Cambrian (Adoudou formation), just above the volcanic formations of the Jbel Boho between Bou Azzer El Graara and Zenaga inliers. The region is by an E-W shortening resulting in an overlapping structure with vergence associated with folds. Generally, the mineralization is hosted along the principal fault of Jbel N'Zourk and sometimes in the anticlines hinges. The petrographic study showed that the mineralization can be observed in several aspects, either in the fractures and veins, in small karsts or rarely disseminated in calcite and dolomite minerals. These observations host new arguments who contribute to a later reconcentration of the copper mineralization of Jbel N'Zourk, trapped on faulted and folded structures attributed to Variscan deformation.

## Keywords

Central Anti-Atlas, Lower Cambrian Cover, Copper Mineralization, Structural

## 1. Introduction

Many copper occurrences are present in the Neoproterozoic-Cambrian cover, also known as the Adoudounian cover [1] (**Figure 1**). These indices are poorly

documented and have generally been considered to be the result of syngenetic processes [2] [3] [4]. The great interest of mining groups in copper resources guides the need for the best constraint of the geological history of such mineralizations. The origin of these ores, which are hosted at different stratigraphic levels of the Adoudounian cover, remains in most cases poorly known even if few of them are currently being mined. Few of these copper orebodies are currently mined. Active mines include the Jbel Laassel mine whose reserves are estimated to be 7,500,000 t with 1% Cu, [5] the Agoujgal mine whose reserves are estimated to be 5,200,000 t with 1.11% Cu and 21 g/t Ag, [6] and the Ouanssimi mine whose reserves are estimated to 1,300,000 t with 2.65% Cu [5]. Other ore bodies are in exploration phase (Jbel N'Zourk, Tarmmant, Tizi N'Mekraz, Assif N'Zaid, Oued Rthem, Tizert...) [2] [5] [6]. The Jbel N'Zourk copper body is the largest copper deposit in the Adoudounian cover in Central Anti-Atlas. It is located at the southern flank of the Central Anti-Atlas between the Bou Azzer El Graara and Zenaga inliers (**Figure 1**). Exploration studies performed by Managem group since 2016, are presently estimating the resources at 1,250,000 t with 1.12% Cu [7]. The aims of the present work are to characterize the copper mineralizations in Jbel N'Zourk, the nature and structural analysis of their host rocks, and the relationships between the mineralized rocks and tectonics structures, Which will contribute to highlight the role of the deformation of the Adoudounian cover in the emplacement of copper mineralizations, based on structural, microstructural, and petro-graphic observations.

## 2. Regional Geological Setting

### 2.1. The Anti-Atlas Belt

Located along the northern border of the WAC (West African Craton) [10], it is limited by the alpine chain of the High Atlas to the North, by the Tindouf basin to the South, by the Atlantic Ocean to the West and by the Tafilet and Bechar basins in the East. It is a large Atasic bulge oriented ENE-WSW, superposed on a Hercynian fold whose anticlinal core reveals the Proterozoic crystalline basement through “inliers” [Bas Drâa, Ifni, Kerdous, Tagragra of Akka, Igherm, Tata, Izazen, Iguerda, Ouzellarh, Sirwa, Zenaga, Bou Azzer el Grara, Saghro and Ougnat] (**Figure 1**), distributed along two major fault zones (South Atlas Fault, and Central Anti-Atlas Fault). This belt has recorded Eburnean, Pan-African and Hercynian orogenesis, which are related to the Paleoproterozoic, Neoproterozoic and Paleozoic respectively. The Precambrian basement is formed by diversified sedimentary and metamorphic complexes, often intruded by granitic complexes dated at  $2050 \pm 10$  MA [11], and more rarely, by basic and ultrabasic intrusive rocks while the Pan-African belt shows ophiolitic complexes are preserved along the Anti-Atlas Major Fault (AAMF) in the Bou Azzer and Siroua inliers [12]-[21]. All these formations are also associated with many acid and basic volcanic rock bodies of variable nature and size. The rest of the Anti-Atlas region is generally covered by Paleozoic terrain rarely deformed [15] [16] [22] [23]

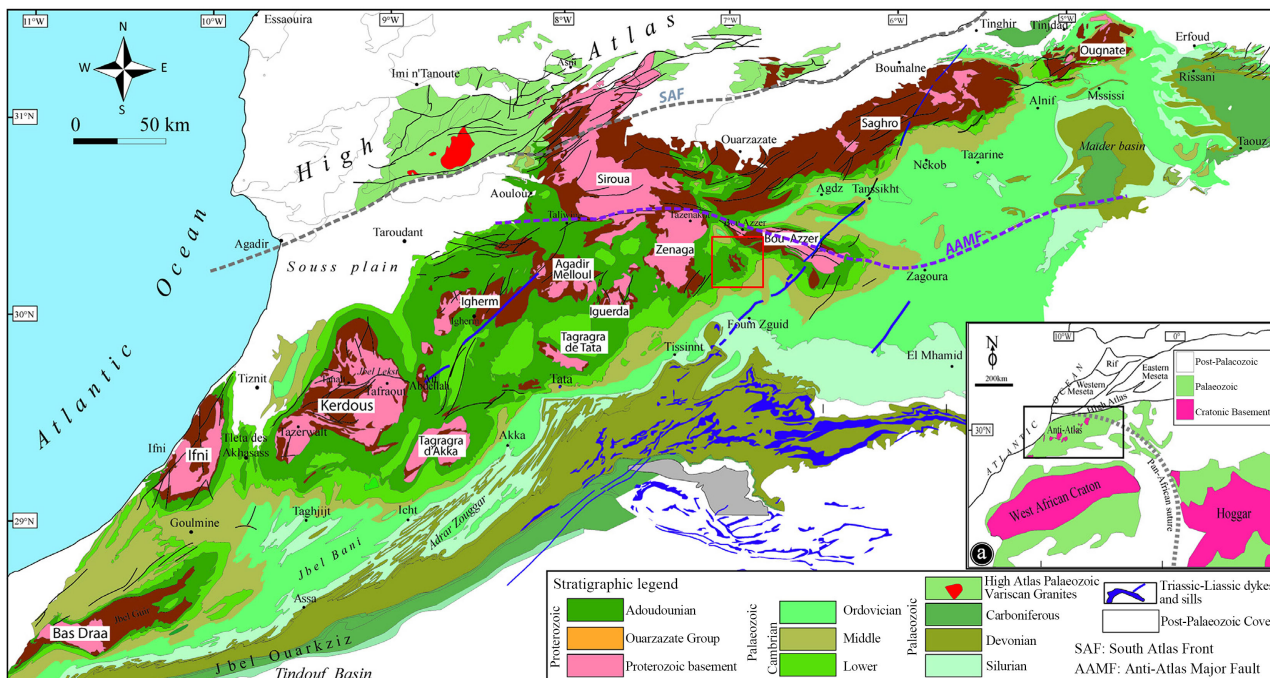


**Figure 1.** Generalized geological map of the Anti-Atlas, simplified from the Geological Map of Morocco, scale 1:1,000,000 [8] [9]; (a): Location of the Anti-Atlas within the structural domains of NW Africa, the studied region is indicated by red square.

[24] [25] [26]. The latter is largely developed on the southern flank of the Anti-Atlas anticlinal [23] [27].

## 2.2. The Adoudou Formation

Its name is related to the Adoudou Oued located to the west of the Anti-Atlas [24]. This formation crops out largely in the Anti-Atlas belt and southwest of the High Atlas with a 1000 m thick series and represents the oldest volcano-clastic complex unconformably covering the Neoproterozoic Ouarzazate group [28] [29]. The Adoudou Formation is associated with a major marine transgression from the West to the Est. It has been subdivided into two groups: the Taroudant Group, with Lower Dolostones and Lower Sandstones units, and the Tata Group, with Upper Dolostones and Upper Sandstones units [23] [30] [31] [32] [33]. The Adoudounian series shows significant variations in facies and thickness. Moving eastward (Saghro, Ougnat, etc.), these series become thinner and dominated by increasingly coarser terrigenous facies, as opposed to the carbonate facies deposited to the west (Tiznit region) [27] [23]. A calico-alkaline volcanism is initiated during the same period as the sedimentation of the Adoudou formation. Two volcanic complexes, Jbel Boho and El Gloa, are located in the Central Anti-Atlas [22] [34] [35]. Old lava flows belonging to the Jbel Boho volcanic system, interspersed in the Adoudou formation, have been dated at  $534 \pm 10$  MA (U/Pb Shrimp on Zircon) [35] and at  $531 \pm 5$  MA [35].

## 3. Local Geological Setting

The Jbel N'Zourk deposit is hosted in the Lower Cambrian part of the late Edia-

caran to Cambrian volcano-sedimentary formations at the southern flank of the Central Anti-Atlas between the Zenaga and Bou Azzer El Graara inliers, 50 km NW of the Bleida mine. Geological mapping, fieldwork and lithological description of drill cores have allowed us to construct the lithostratigraphic column of the Jbel N'Zourk region (**Figure 2 & Figure 3**), which consists of a thick succession (approximately 800 m) of the Adoudounian cover. We distinguish from bottom to top:

- The basal series: represented in the studied region by a breccia and conglomeratic unit with a thickness of 5 to 100 meters, composed of subangular elements which origin is the underlying volcano-sedimentary series. Horizontal rough bedding appears locally in these facies, indicating a high energy deposition process in a fan-delta system.
- The lower limestone: with a 150 - 250 m thickness series composed of a succession of dolomitic limestones levels separated by red and white clays siltstones showing some local breccia recurrences. The dolomitic levels, when they are not massive, are frequently characterized by the presence of horizontal laminates of microbial origin and more rarely by stromatolitic domed structures. Intense secondary silicifications affect the dolomites in Jbel N'Zourk.
- The Jbel Boho volcanic complex: with levels of pyroclastic tuffs, lava and volcanic breccias interspersing at the base of the lower limestones in Jbel N'Zourk. These volcanic manifestations are mainly found in the river area (Mechkerj River). This volcano-sedimentary series with a thickness varying from 100 to 200 m indicates a synsedimentary volcanic system, which was to constitute an emerging relief, with dismantling products transported in the form of debris flows interbedded within the platform deposits of the Adoudounian formation.

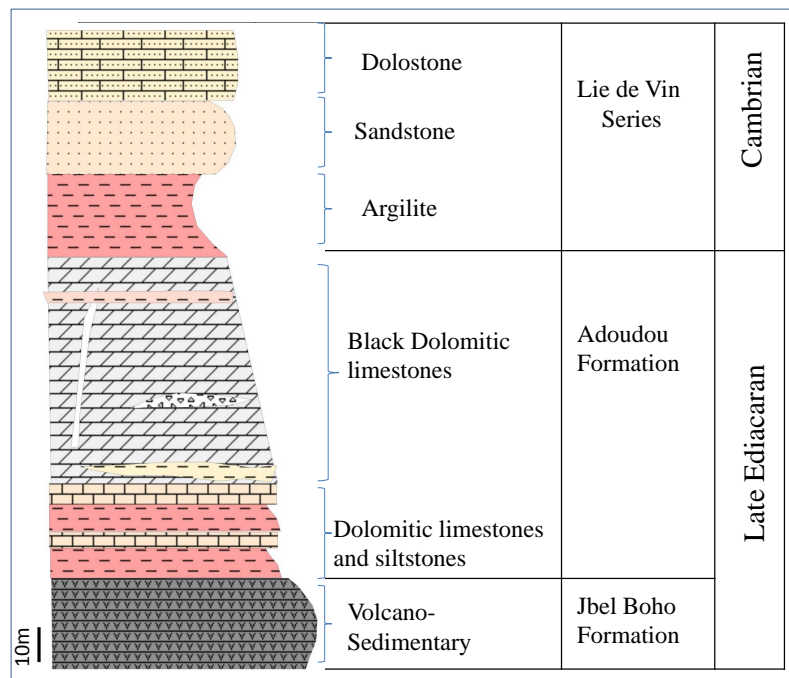


**Figure 2.** Lithostratigraphic columns of the Jbel N'Zourk area.

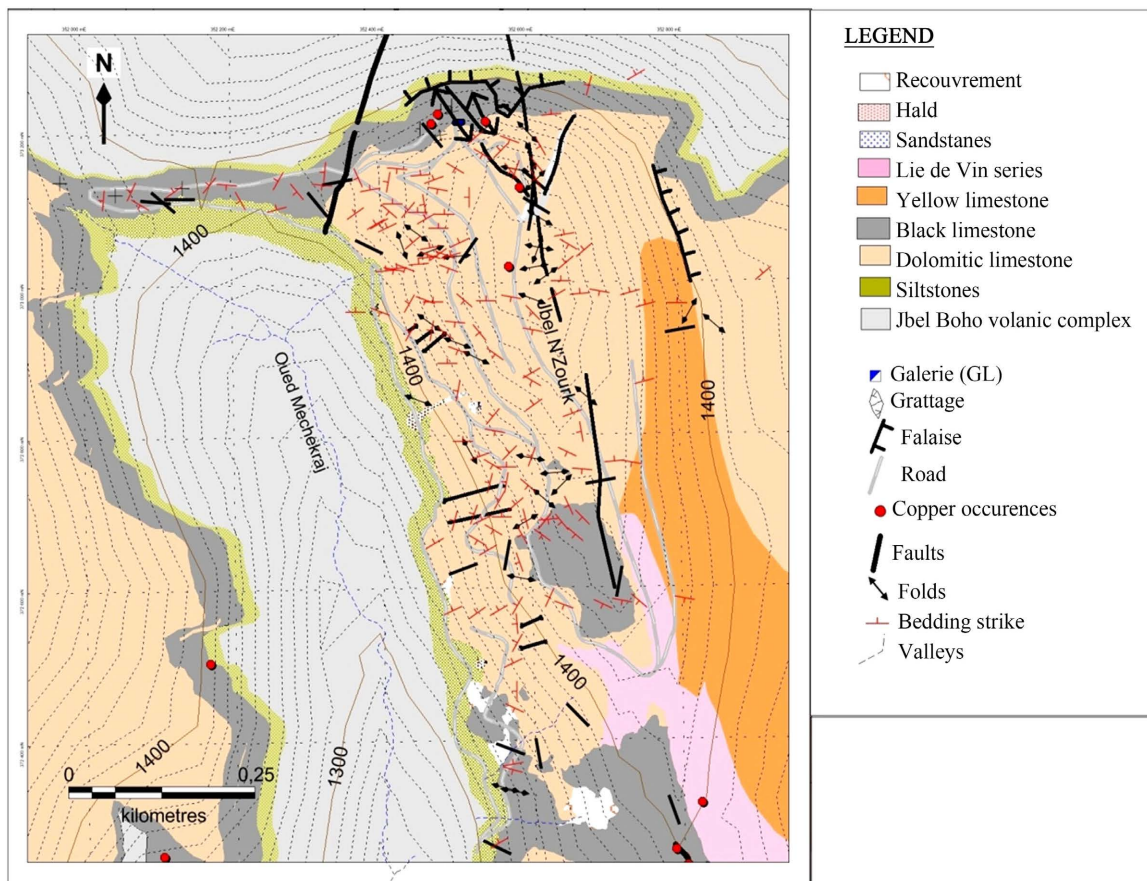


**Figure 3.** Geological and structural map of the Jbel N'Zourk area.

- The “Lie de Vin” Series: are lower sandstones that are part of the Tikirt Formation (150 to 200 m thick) which is composed essentially by a red clays-tones of sand-stones frequently interlayered by centimetric clayed siltstones and purple argillites representing a significant sea level regression.

The vertical change in facies from the lower limestone to the “Lie de Vin” series is rapid and progressive; on the other hand, this series is brutally surrounded, without any visible discordance, by the upper limestones, which initiates a new negative sedimentary sequence.

#### 4. Sampling and Analytical Methods

In order to establish a detailed survey of the Jbel N'Zourk copper mineralized veins and to understand their distribution and tectonic control, a structural and microstructural study has been performed in the prospect area. Samples were collected from outcrops and drill cores were used for petrographical, mineralogical, and geochemical studies. Polished thin sections were prepared from these samples and have been first studied using a petrographic microscope with transmitted and reflected light modes. Complementary observations and mineral's analyses were carried out using JSM IT100 (JEOL) Scanning Electron Microscope (SEM) with 0.5 to 30 kV accelerating voltage. The SEM system is

coupled to Energy-Dispersive X-ray fluorescence (XRF) spectrometer (EDS) to make qualitative compositions of sulphide minerals from ten polished sections. Whole-rock geochemical data of samples collected at different prospect area were determined at the Reminex Research Center (MANAGEM Group). For the major elements analysis ( $\text{SiO}_2$ ,  $\text{Al}_2\text{O}_3$ ,  $\text{Fe}_2\text{O}_3$ ,  $\text{CaO}$ ,  $\text{MgO}$ ,  $\text{MnO}$ ,  $\text{K}_2\text{O}$ ,  $\text{TiO}_2$ ,  $\text{P}_2\text{O}_5$ ), 0.5 g of the sample is crushed at less than 100  $\mu\text{m}$  and it is dissolved by fusion at 500°C during 40 min with 2.5 g of sodium peroxide in a zirconium crucible. The melt mixing is then dissolved with 100 mL of hydrochloric acid (28% HCl) and the solution is analyzed using an ICP-AES ULTIMA 2C using the Jobin Yvon-HORIBA device. For the other elements (Cu, CuOx, As, B, Ba, Be, Bi, Cd, Co, Cr, Ge, Li, Mo, Nb, Ni, Pb, Sb, Se, Sn, Sr, W, Y, Zn, Ag), 0.25 g of the sample is dissolved by microwave-assisted acid attack (50% HCl and 50%  $\text{HNO}_3$ ) during 40 min at 220°C. The solution is then analyzed by ICP-MS Thermo X'Serie 2.

## 5. Results

### 5.1. Structural Study

The Jbel N'Zourk area is located in a large anticlinal structure. This structure only affects the higher terms compared to the basic silty sandstone and ferruginous micro-conglomerates. The whole sequence in Jbel N'Zourk undergoes at least two deformation stages. Two types of folds are present. The first family corresponds to very tight folds characterized by axial planes poured eastward or kneeling folds, with an N-S orientation. Fracture schistosity, absorbed essentially by the levels of siltstones between dolomitic limestones, is associated with these folds. The second fold family characterized by very open is opaque folds oriented NE-SW; of pluri-metric to plurikilometric amplitude spatially associated with overlaps of the same direction, and are distributed mainly in the western flank of Jbel N'Zourk. Sometimes we can observe in the same folding axis the passage from tight folds to kneeling folds. This disharmony is due to the effect of discontinuity and variability in the power of the siltite levels between the limestones. These silty horizons played a soapy role when the limestone bars were folded. Some of these folds are therefore interpreted as fault propagation folds that have formed at the tip of blind thrust and back thrust that terminate upward from a flat decollement localized along the upper boundary of the Jbel Boho formation.

One decametric extension thrust fault can be observed at the top of the Jbel N'Zourk relief, where the unit of the lower dolomitic limestones in underlying the unit of siltstones and sandstones of the series of "Lie de Vin", along a NNW-SSE trending thrust dipping 80° to the east (Figure 4 and Figure 5).

The western flank of Jbel N'Zourk is the most deformed part; the survey of the fracturing made it possible to distinguish two families of faults, a NNW-SSE orientation family that generally ranges from N150° and N180°, parallel to the major Jbel N'Zourk fault, and a second E-W family characterized by an orientation between 45° and N 70° (Figure 6).

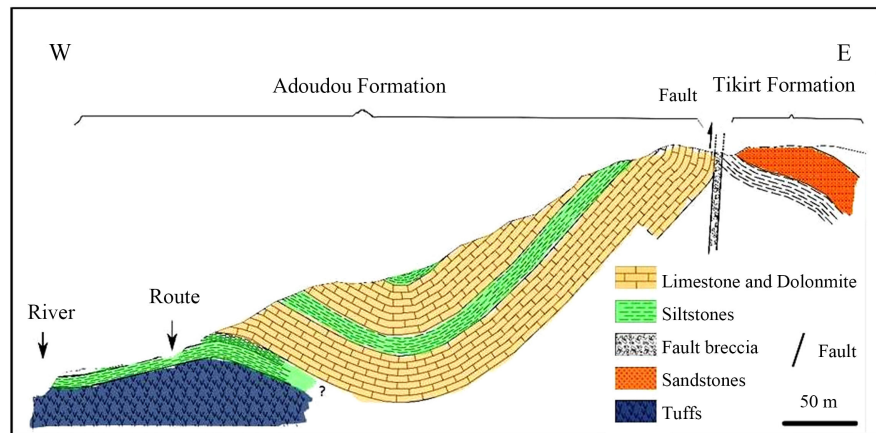


**Figure 4.** Geological cross section showing the structure of the Jbel N'Zourk deposit.

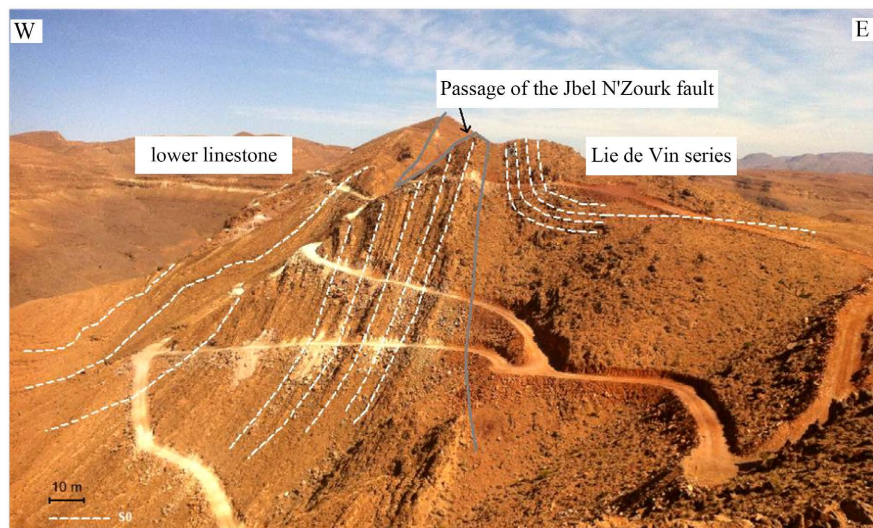


**Figure 5.** Panoramic view showing the passage of the Jbel N'zourk fault in the study area.

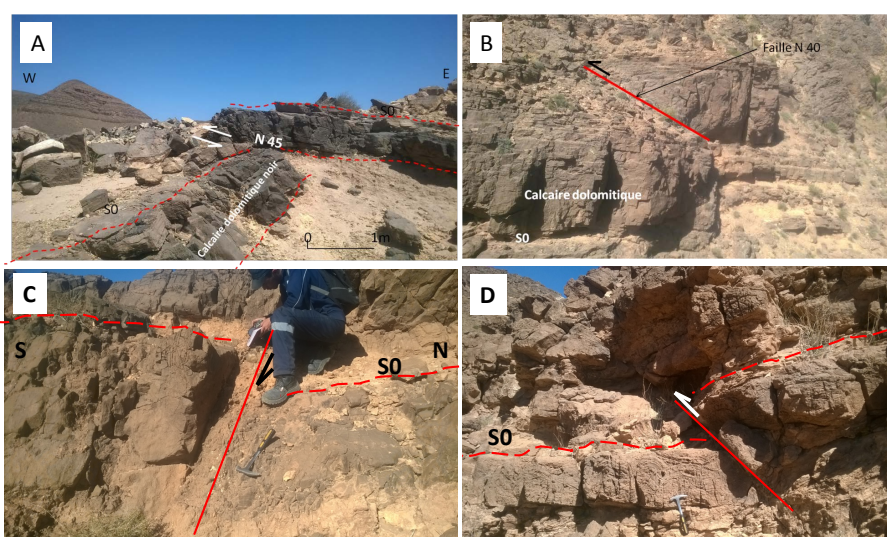


**Figure 6.** Fracturing in the study area: (A) reverse fault N45; (B) reverse fault N40; (C) normal fault at the crest of Jbel N'Zourk; (D) reverse fault on the western flank of Jbel N'Zourk.

In addition to the large structures of Jbel N'Zourk, microstructures have been identified within the mineralization, which essentially corresponds to veins, veinlets, microfails, tension slots and veins (**Figure 7**).

These microstructures sometimes show indications that provide information on the movement and cinematic properties of the tectonic deformations that have affected the region. Jbel N'Zourk is a region characterized by intense fracturing that sometimes makes the entire structure difficult to identify due to large scree overlaps (**Figure 7**).

## 5.2. Copper Mineralization

### 5.2.1. Geometries and Orientation

In the Jbel N'Zourk copper deposit, the economic mineralized zone is present in the western part of the Jbel N'Zourk fault in a thick series of carbonates of the Adoudou formation. The sulphides are mainly hosted in the base of the lower carbonate formation in veins and sometimes in the base siltstones of the series. The lateral and vertical extent of ore bodies was delimited by cartography and drilling studies. The thickness of the mineralized zone reaches 40 m. Locally,

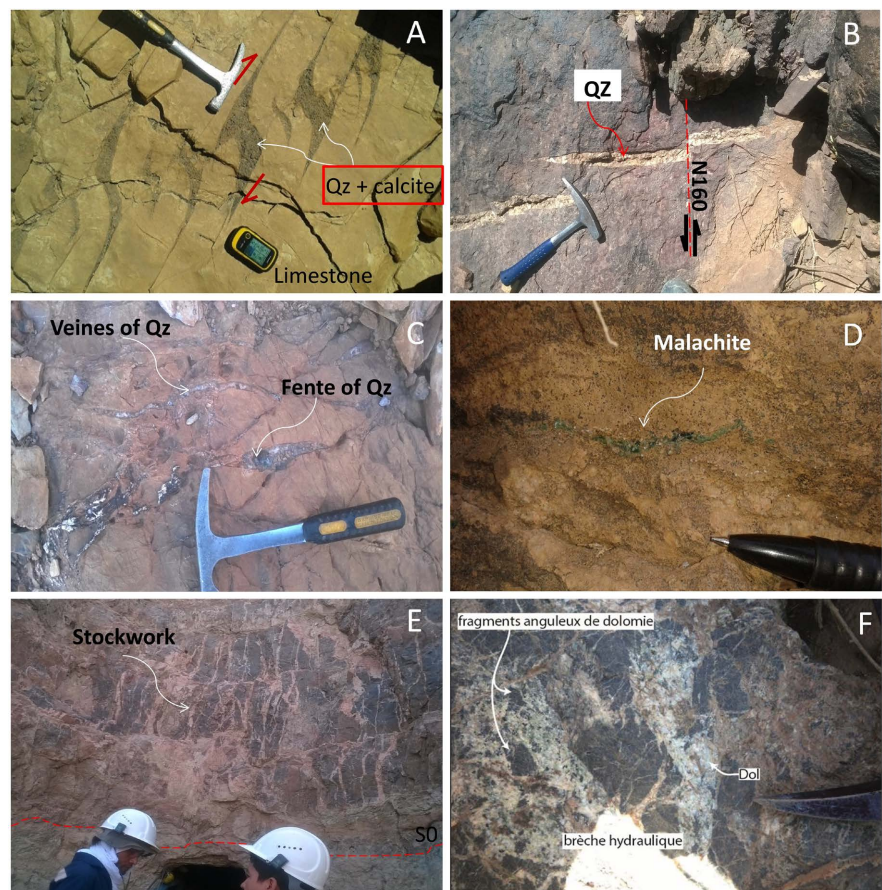


**Figure 7.** Photographic view of micro-structures at Jbel N'zourk. (A) sigmoidal Z tension fractures; (B) micro-fault in the Jbel Boho volcanic formation; (C) quartz veins and fractures; (D) malachite vein; (E) Stockwork secant on stratification; (F) hydraulic breccias with angular fragments.

later copper sulphide minerals are distributed in both families of the faults NNW-SSE and E-W in the Adoudou formation. In this formation, sulphides occurrence are essentially observed in fractures, in quartz veins and in quartz and calcite geodes. The eastern boundary of ore bodies present the Jbel N'Zourk fault zone, the southern and western boundaries of the deposit are not explored and are not yet fully defined, but ongoing drilling exploration activities aim to define the boundaries of the economic mineralized zones in this deposit.

### **5.2.2. Associated Mineralogy and Paragenetic Succession**

Without distinction between primary and secondary origin, the copper mineralization in Jbel N'Zourk deposit is composed of bornite, calcocite, chalcopyrite, covellite, pyrite, digenite, malachite, azurite, cuprite, tenorite and chrysocolla, associated with quartz, dolomite and calcite as gangue mineral. This mineral gangue in the veinlets or voids systematically has a banding texture. When these three phases are present, it forms ribbons within the veins with quartz on the epones, then dolomite and finally calcite in the center. This gangue chronology is a great reference point for determining the succession of copper minerals in this deposit. Bornite is the most abundant and developed copper sulphide in the deposit as evidenced by petrographic observations (**Figures 8(A)-(C)**), being partially or totally replaced by calcocite. Chalcopyrite often appears as a corona around the bornite and rarely included in the bornite (**Figure 8(A)**, **Figure 8(C)**). This association can be explained by exsolution between the two phases or by the replacement of the bornite by chalcopyrite. Chalcopyrite and bornite are transformed into dark blue colored covellite, digenite and calcocite (**Figure 8(A)**, **Figure 8(B)**). These secondary alteration minerals are observed mainly in the rims of the bornite and chalcopyrite minerals. However some Cristals can be totally replaced by late calcocite, digenite and covellite. The mineral phases of copper carbonates are generally associated with the supergenic alteration of primary sulphides and are composed of malachite, azurite and chrysocolla (**Figures 8(D)-(F)**). These copper carbonates are present as secant veinlets on all structures replacing sulphides and dolomites. All these relationships between minerals allow the distinction of a primary paragesesis represented by: quartz, bornite, chalcopyrite, dolomite and calcite, and a secondary one represented by: covellite, calcocite, digenite, malachite, azurite, chrysocolla, tenorite and cuprite. Based on the intersection relationships between the different mineral phases, several episodes of fracturing have been observed (**Figure 8; Table 1**).

### **5.2.3. Multiscale Observations of the Ore Texture**

In the field and at macroscopic scale, two types of textural mineralization have been identified; the most frequent texture of mineralization in ore deposit is a stockwork with veins, fractures and veinlets are oblique to the stratification. The veins of this stockwork have locally combed quartz textures. The second type of texture corresponds to disseminations within the rock groundmass in the basic siltstones. Locally it is spatially related with the stockwork texture. At the micro-

scopic scale by observation of polished thin sections, both types of mineralization appear composed by the same ore and gangue minerals. Textural, chronological relationships and paragenetic sequence has being also similar (**Figure 8**).

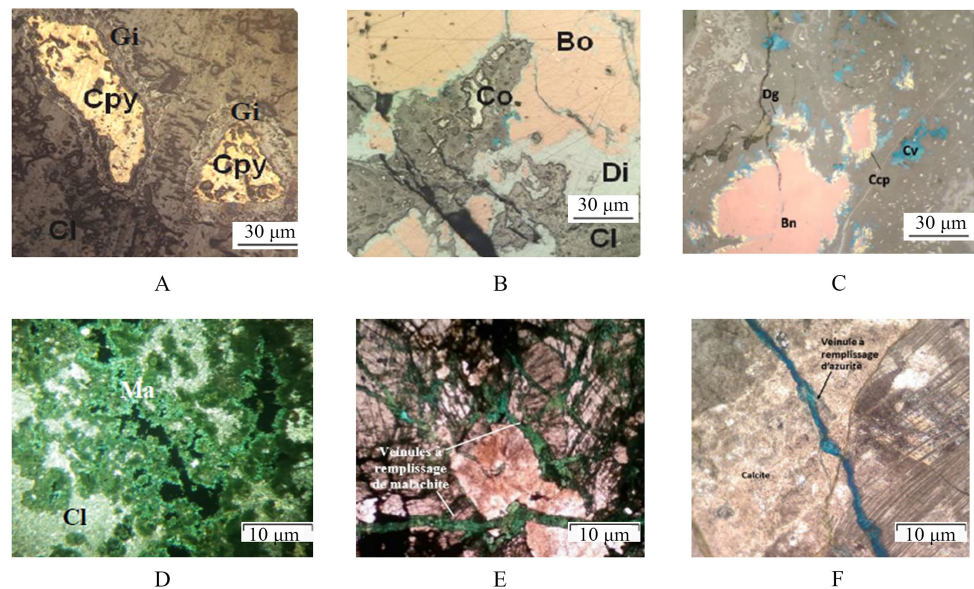


**Figure 8.** Paragenetic associations and replacement textures. (A) Disseminated chalcopyrite (Cpy), associated with Gitite (Gi) and calcite (Cl); (B) Vein of bornite (Bn), covellite (Cv), digenite (Dg) and calcite (Cl); (C) bornite replaced by chalcopyrite; (D) “Peigne texture”; (E) Malachite veinlets; (F) Azurite veinlets.

**Table 1.** Paragenetic succession of the Jbel N’Zourk deposit.

Minerals	Primary assemblage	Secondary assemblage
Quartz ( $\text{SiO}_2$ )	●	
Dolomite ( $\text{CaMg}(\text{CO}_3)_2$ )	●	
Calcite ( $\text{CaCO}_3$ )	●	
Chalcopyrite ( $\text{CuFeS}_2$ )	●	
Bornite ( $\text{Cu}_5\text{FeS}_4$ )	●	
Chalcocite ( $\text{Cu}_2\text{S}$ )		●
Digenite ( $\text{Cu}_9\text{S}_5$ )		●
Covellite ( $\text{CuS}$ )		●
Malachite ( $(\text{Cu}_2)_2\text{CO}_3(\text{OH})_2$ )		●
Azurite ( $\text{Cu}_3(\text{CO}_3)_2(\text{OH})_2$ )		●
Natif copper (Cu)		●
Chrysocolla ( $(\text{Cu},\text{Al})_2\text{H}_2\text{SiO}_5(\text{OH})_4$ )		●
	→ Fissuring	

### 5.2.4. Principal Component Analysis (PCA) of Chemical Data

The database of the JBEL N'ZOURK prospect is composed of 97 samples that correspond to the sampling by lithology of the copper mineralized zone (**Table 2** and **Table 3**). This database contains analyses of Total copper (Cu) (**Figure 9**). The results of the PCA show that two factors F1 and F2 explain 60.07% of the total variability (**Figure 10(A)**). Three groups of elements discriminated in the F1 - F2 plane (**Figure 10(C)**) corresponding in the observation plan to siltstones, dolostones and potentially to tectonic breccias for the group represented by the rare elements (**Figure 10(D)**). The copper variable, not well represented in the F1 - F2 plane, would be considered to have an affinity for the siltstone group (**Figure 10(D)**). This representation of the variables suggests that copper is not related to any of the three types of lithology. Indeed, copper is independent of sedimentary siltstones and dolostones, and it is anticorrelated with the lavas formation. The factors F2 and F5 are the most correlated with the copper variable (**Figures 10(D)-(F)**). Moreover, an examination of the F2 - F5 plane, suggests that copper could be associated with titanium, with correlation coefficient between total copper and titanium is 0.62 (**Figure 10(E)**, **Figure 10(F)**). In a binary representation, the coefficient of determination, between these two elements, is 0.4 which shows that the correlation between these two elements is limited (**Figure 9**). Therefore, the PCA highlights the independence of copper (total and oxidized) relative to the others variables present in the available database, especially that corresponding to lithology (**Figure 10**).

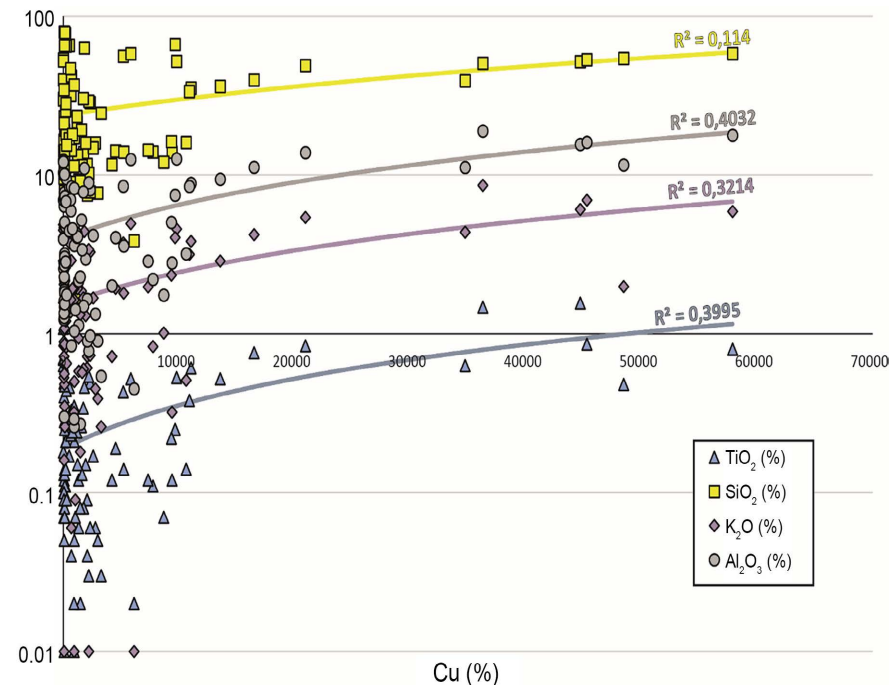


**Figure 9.** Binary graph showing  $\text{TiO}_2$ ,  $\text{SiO}_2$ ,  $\text{K}_2\text{O}$  and  $\text{Al}_2\text{O}_3$  content as a function of total copper (Cu) content. The straight lines correspond to the regression lines, their colors to the different variables compared to the copper contents.  $R^2$  is the coefficient of determination. The ordinate scale is logarithmic.

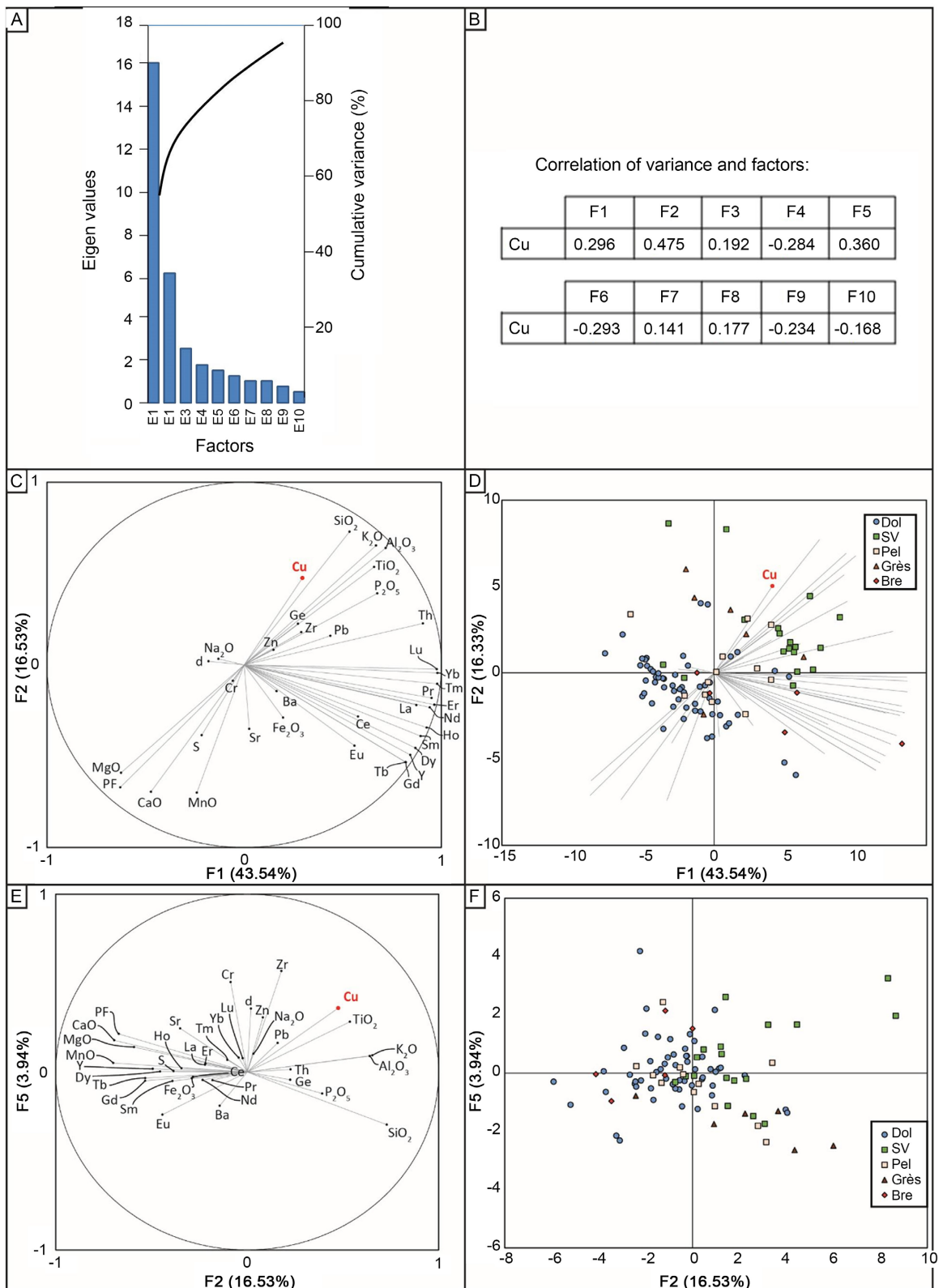


**Figure 10.** Results of PCA analyses of the database of Jbel N'Zourk deposit. (A) Eigenvalues and cumulative variance function of factors. (B) Table of correlation between the copper variable and the factors. (C) Variables projection in the F1 - F2 plane. (D) Samples lithology project in F1 - F2 plane. (E) Variables projection in the F2 - F5 plane. (F) Samples lithology project in F2 - F5 plane.

**Table 2.** Whole rock major element chemical data of the studied samples from the Jbel N'Zourk deposit.

Sample	Rock type	SiO <sub>2</sub>	Al <sub>2</sub> O <sub>3</sub>	Fe <sub>2</sub> O <sub>3</sub>	CaO	MgO	K <sub>2</sub> O	MnO	TiO <sub>2</sub>	P <sub>2</sub> O <sub>5</sub>	Na <sub>2</sub> O
JNZ 01	Siltstone	51.92	12.86	2.43	9.15	3.85	4.55	0.16	0.55	0.13	0.43
JNZ 02	Dolostone	13.28	4.09	2.34	24.6	14.92	1.93	0.56	0.14	0.05	0.32
JNZ 03	Dolostone	64.84	9.43	2.65	6.34	2.54	4.14	0.16	0.45	0.15	0.36
JNZ 04	Siltstone	57.93	12.52	3.25	6.34	3.06	4.94	0.14	0.54	0.15	0.37
JNZ 05	Dolostone	16.94	4.43	2.58	24.25	13.53	1.85	0.47	0.16	0.08	0.22
JNZ 06	Dolostone	65.35	10.06	2.55	5.75	2.46	4.18	0.13	0.46	0.17	0.34
JNZ 07	Siltstone	63.05	10.98	3.16	3.69	4.77	4.46	0.15	0.47	0.14	0.47
JNZ 08	Dolostone	11.13	3.06	2.76	25.93	15.74	1.45	0.52	0.15	0.05	0.22
JNZ 09	Siltstone	41.93	8.42	2.85	14.44	7.22	2.86	0.24	0.34	0.12	0.53
JNZ 10	Dolostone	12.93	2.73	2.34	26.63	15.28	0.57	0.45	0.15	0.04	0.54
JNZ 11	Dolostone	77.44	6.84	1.06	4.42	0.94	2.64	0.16	0.15	0.06	0.14
JNZ 12	Breccia	36.34	8.24	1.55	25.43	1.43	1.93	0.17	0.34	0.11	0.48
JNZ 13	Dolostone	8.95	1.45	1.48	28.03	17.04	0.08	0.33	0.06	0.03	0.56
JNZ 14	Dolostone	15.95	3.16	1.55	24.44	15.03	0.54	0.24	0.15	0.04	0.62
JNZ 15	Dolostone	30.43	6.96	1.46	18.03	10.04	2.85	0.14	0.68	0.07	0.16
JNZ 16	Siltstone	13.83	1.48	3.23	35.44	7.73	0.66	0.23	0.09	0.13	0.14
JNZ 17	Dolostone	7.68	0.92	1.84	27.34	18.05	0.36	0.24	0.06	0.03	0.15
JNZ 18	Dolostone	29.66	3.93	1.64	27.38	12.96	1.56	0.24	0.17	0.03	0.13
JNZ 19	Dolostone	15.93	1.34	2.35	27.74	13.54	0.46	0.35	0.07	0.05	0.18
JNZ 20	Siltstone	19.24	5.24	1.93	31.25	6.76	1.86	0.26	0.27	0.13	0.24
JNZ 21	Siltstone	53.85	12.27	1.72	9.36	3.53	4.06	0.18	0.74	0.18	0.16
JNZ 22	Dolostone	14.84	4.14	2.53	25.47	13.63	1.69	0.47	0.18	0.08	0.14
JNZ 23	Breccia	23.34	4.05	2.34	27.65	8.66	1.38	0.37	0.24	0.12	0.15
JNZ 24	Dolostone	25.32	4.76	1.75	22.96	16.56	1.93	0.48	0.22	0.12	0.17
JNZ 25	Dolostone	6.73	1.81	1.86	23.22	13.78	0.63	0.63	0.08	0.05	0.17
JNZ 26	Dolostone	11.04	3.17	1.96	27.34	14.43	1.07	0.46	0.15	0.07	0.19
JNZ 27	Dolostone	64.93	7.71	1.46	10.15	1.34	3.12	0.15	0.27	0.16	0.18
JNZ 28	Siltstone	13.24	2.2	2.46	25.66	15.96	0.83	0.43	0.07	0.08	0.17
JNZ 29	Dolostone	7.86	1.48	3.05	27.35	16.55	0.64	0.63	0.08	0.07	0.17
JNZ 30	Dolostone	19.18	5.07	2.55	22.16	13.77	1.76	0.44	0.26	0.12	0.13
JNZ 31	Siltstone	31.64	5.95	1.65	27.85	3.52	1.65	0.23	0.27	0.13	0.22
JNZ 32	Dolostone	15.94	2.96	2.06	26.5	13.63	1.35	0.43	0.16	0.07	0.13
JNZ 33	Siltstone	52.12	12.25	1.97	8.8	5.44	4.85	0.12	0.63	0.18	0.16
JNZ 34	Dolostone	24.53	0.55	1.98	21.76	14.87	0.26	0.33	0.04	0.02	0.43
JNZ 35	Siltstone	53.14	16.14	1.58	4.5	2.75	6.94	0.06	0.85	0.14	0.75
JNZ 36	Dolostone	1.66	0.28	2.97	30.06	18.12	0.17	0.45	0.03	0.03	0.37

**Continued**

JNZ 37	Siltstone	50.66	18.94	1.57	3.3	2.9	8.66	0.56	1.46	0.18	0.94
JNZ 38	Dolostone	17.96	2.93	1.68	23.4	15.53	0.84	0.26	0.23	0.09	0.28
JNZ 39	Dolostone	9.26	1.14	1.99	25.46	18.45	0.55	0.35	0.06	0.03	0.52
JNZ 40	Siltstone	39.05	11.44	2.08	12.13	7.33	4.36	0.16	0.65	0.08	0.52
JNZ 41	Dolostone	8.25	1.04	1.59	26.24	18.84	0.56	0.65	0.04	0.04	0.32
JNZ 42	Breccia	34.34	9.95	4.46	22.06	1.84	4.67	0.12	0.48	0.12	0.32
JNZ 43	Siltstone	79.23	7.24	1.03	2.84	0.84	4.13	0.04	0.14	0.12	0.44
JNZ 44	Siltstone	65.44	8.41	2.68	8.04	1.25	3.73	0.15	0.46	0.13	0.42
JNZ 45	Siltstone	30.26	7.66	1.24	29.95	1.43	1.65	0.14	0.35	0.13	0.68
JNZ 46	Breccia	11.44	3.34	1.07	44.15	1.07	0.56	0.14	0.14	0.07	0.65
JNZ 47	Dolostone	14.25	0.86	1.73	27.23	15.16	0.07	0.25	0.03	0.04	0.56
JNZ 48	Dolostone	12.34	1.43	1.58	27.33	16.14	0.28	0.25	0.07	0.03	0.54
JNZ 49	Dolostone	14.24	1.81	1.58	25.04	16.05	0.38	0.17	0.07	0.05	0.64
JNZ 50	Dolostone	10.36	1.28	1.77	27.23	17.16	0.16	0.16	0.06	0.03	0.43
JNZ 51	Dolostone	21.13	0.32	1.44	26.04	13.57	0.05	0.14	0.03	0.04	0.42
JNZ 52	Siltstone	78.74	7.33	1.06	3.95	0.88	2.14	0.13	0.14	0.07	0.17
JNZ 53	Siltstone	46.65	6.97	1.33	22.34	0.65	1.37	0.16	0.24	0.07	0.24
JNZ 54	Siltstone	54.07	11.56	1.38	7.33	3.76	1.96	0.24	0.47	0.06	0.34
JNZ 55	Dolostone	10.25	0.79	1.45	26.34	17.28	0.02	0.44	0.02	0.03	0.49
JNZ 56	Breccia	28.15	6.77	1.55	28.4	3.79	1.22	0.16	0.26	0.06	0.56
JNZ 57	Dolostone	13.92	2.79	1.84	25.75	13.76	0.22	0.27	0.13	0.02	0.36
JNZ 58	Dolostone	3.84	0.48	2.73	24	18.57	0.11	0.35	0.03	0.02	0.65
JNZ 59	Dolostone	4.34	0.27	1.35	28.95	19.64	0.01	0.25	0.03	0.02	0.48
JNZ 60	Dolostone	13	1.62	1.88	25.36	17.76	0.82	0.17	0.12	0.02	0.66
JNZ 61	Dolostone	10.73	1.35	1.67	25.86	17.66	0.73	0.17	0.08	0.03	0.38
JNZ 62	Dolostone	14.14	4.04	2.49	25.17	13.76	1.93	0.37	0.18	0.02	0.46
JNZ 63	Dolostone	18.33	2.22	1.41	25.77	15.88	0.47	0.18	0.12	0.09	0.69
JNZ 64	Dolostone	9.51	1.24	2.77	26.88	16.78	0.54	0.4	0.08	0.06	0.23
JNZ 65	Siltstone	23.26	6.48	1.75	29.67	6.13	2.05	0.14	0.42	0.14	0.17
JNZ 66	Dolostone	16.53	2.71	1.87	27.55	16.34	1.06	0.13	0.12	0.06	0.21
JNZ 67	Dolostone	14.13	2.56	2.22	24.42	16.05	0.85	0.14	0.13	0.06	1.42
JNZ 68	Dolostone	17.12	3.66	2.35	27.46	11.16	1.66	0.25	0.22	0.13	0.42
JNZ 69	Dolostone	21.46	4.24	2.65	27.52	8.86	2.07	0.26	0.25	0.12	0.365
JNZ 70	Dolostone	35.18	8.74	2.14	17.35	7.47	3.83	0.24	0.62	0.14	0.13
JNZ 71	Dolostone	11.62	1.55	1.55	26.51	16.76	0.65	0.25	0.08	0.06	0.12
JNZ 72	Siltstone	39.53	11.37	2.35	14.16	6.54	4.25	0.17	0.75	0.18	0.23
JNZ 73	Dolostone	13.93	2.24	1.76	26.35	15.35	0.84	0.25	0.12	0.06	0.27
JNZ 74	Siltstone	55.74	8.45	1.06	12.11	3.05	3.75	0.08	0.42	0.15	0.04

**Continued**

JNZ 75	Siltstone	51.65	15.53	1.55	6.12	2.18	6.06	0.08	1.55	0.3	0.03
JNZ 76	Dolostone	11.62	2	1.64	27.32	15.76	0.77	0.17	0.13	0.06	0.16
JNZ 77	Siltstone	36.05	9.36	1.72	19.72	5.05	2.85	0.27	0.51	0.17	0.14
JNZ 78	Siltstone	28.56	8.05	1.65	28.78	2.76	3.26	0.08	0.48	0.17	0.07
JNZ 79	Siltstone	48.7	13.9	2.04	8.98	4.54	5.45	0.08	0.85	0.18	0.02
JNZ 80	Dolostone	29.13	8.94	2.95	25.57	3.04	3.38	0.16	0.56	0.19	1.24
JNZ 81	Siltstone	12.44	2.16	2.43	27.95	13.45	0.95	0.25	0.13	0.08	0.74
JNZ 82	Siltstone	39.58	10.33	1.17	14.24	8.34	4.45	0.15	1.07	0.12	0.22
JNZ 83	Dolostone	11.13	2.82	3.07	26.55	14.97	1.35	0.37	0.15	0.02	0.44
JNZ 84	Dolostone	10.63	1.55	2.25	27.06	16.08	0.84	0.3	0.06	0.02	0.33
JNZ 85	Dolostone	66.15	7.47	2.15	7.67	1.42	4.04	0.12	0.26	0.05	0.12
JNZ 86	Siltstone	16.23	5.03	2.65	23.08	13.83	2.33	0.38	0.23	0.06	0.47
JNZ 87	Dolostone	9.14	2.26	2.26	27	16.42	1.34	0.8	0.07	0.05	0.18
JNZ 88	Dolostone	12.06	1.77	2.25	25.5	15.83	1.03	0.37	0.06	0.05	0.52
JNZ 89	Siltstone	58.08	17.75	1.97	2.26	2.26	5.87	0.07	0.78	0.04	0.15
JNZ 90	Siltstone	13.95	3.56	1.76	24.73	15.13	1.84	0.26	0.15	0.03	0.66
JNZ 91	Dolostone	14.36	2.87	1.97	24.13	15.64	1.94	0.6	0.13	0.04	0.55
JNZ 92	Dolostone	7.46	0.97	2.83	28.51	16.44	0.74	0.37	0.05	0.05	0.13
JNZ 93	Dolostone	17.93	4.58	0.84	38.12	1.63	1.93	0.08	0.25	0.06	0.44
JNZ 94	Dolostone	7.45	0.98	2.15	26.81	18.04	0.73	0.32	0.05	0.04	0.55
JNZ 95	Dolostone	33.45	8.48	1.93	22.59	3.84	3.14	0.08	0.37	0.07	0.33
JNZ 96	Siltstone	15.46	1.78	1.84	24.13	15.53	0.65	0.14	0.08	0.05	0.45
JNZ 97	Dolostone	11.32	0.27	1.85	25.33	17.53	0.34	0.28	0.03	0.04	0.34

**Table 3.** Whole rock trace element chemical data of the studied samples from the Jbel N'Zourk deposit.

Sample	Rock type	Ba	Cr	Cu	Pb	Sr	Zn	Ge	Zr	Y	La	Ce	Pr
JNZ 01	Siltstone	227	28	9796	35	56	11	90	126	13.33	0.63	36.12	5
JNZ 02	Dolostone	158	8	1224	25	96	6	35	76	11.85	10.96	24.57	2.56
JNZ 03	Dolostone	207	22	262	47	44	14	83	86	8.83	9.83	25.14	2.55
JNZ 04	Siltstone	224	25	5834	34	61	12	114	124	10.34	13.72	30.36	3.36
JNZ 05	Dolostone	136	7	498	43	77	12	40	55	12.54	9.06	19.79	2.16
JNZ 06	Dolostone	253	21	94	41	48	13	96	113	10.43	11.09	25.59	2.96
JNZ 07	Siltstone	202	23	1812	30	63	12	72	102	8.12	8.95	21.55	2.48
JNZ 08	Dolostone	96	8	98	31	91	5	34	57	21.95	15.23	34.12	3.64
JNZ 09	Siltstone	167	16	686	60	64	13	365	262	14.88	15.57	38.03	3.76
JNZ 10	Dolostone	217	21	78	56	132	27	167	208	12.94	10.74	25.83	2.68
JNZ 11	Dolostone	548	38	177	72	53	9	160	212	7.83	8.12	17.15	2.28

**Continued**

JNZ 12	Breccia	586	41	934	69	208	10	123	373	14.33	17.16	33.36	3.74
JNZ 13	Dolostone	792	18	1032	34	205	10	74	83	10.64	6.84	103.4	1.78
JNZ 14	Dolostone	121	22	10,617	66	137	13	78	193	10.52	7.93	17.68	2.13
JNZ 15	Dolostone	216	37	4	35	144	198	33	124	10.04	8.92	18.87	2.27
JNZ 16	Siltstone	375	27	1753	37	166	78	151	66	9.04	9.47	27.33	2.44
JNZ 17	Dolostone	74	24	2966	35	97	45	87	122	5.56	6.65	14.64	1.62
JNZ 18	Dolostone	174	31	3	34	105	44	56	185	6.94	7.76	16.45	1.98
JNZ 19	Dolostone	494	25	2772	31	125	33	67	196	7.23	5.58	12.64	1.56
JNZ 20	Siltstone	436	35	1565	37	175	35	33	63	8.24	9.23	32.36	2.24
JNZ 21	Siltstone	381	55	3	31	85	36	54	186	10.54	12.14	26.38	3.14
JNZ 22	Dolostone	387	32	2584	27	134	28	34	67	11.15	10.65	22.39	2.56
JNZ 23	Breccia	445	32	1186	27	203	25	32	154	9.74	8.36	16.97	1.98
JNZ 24	Dolostone	294	32	196	35	131	24	37	168	14.76	11.42	25.56	2.74
JNZ 25	Dolostone	142	24	85	30	117	38	79	223	9.84	7.53	16.28	1.74
JNZ 26	Dolostone	174	28	96	31	113	31	37	55	20.04	17.12	41.76	4.48
JNZ 27	Dolostone	287	37	72	43	54	48	57	86	6.33	6.54	15.75	1.93
JNZ 28	Siltstone	104	27	64	35	103	38	40	78	11.35	9.23	21.56	2.28
JNZ 29	Dolostone	123	25	82	28	114	46	42	67	9.98	6.63	14.69	1.63
JNZ 30	Dolostone	363	31	102	42	135	34	43	86	13.85	10.13	28.54	2.56
JNZ 31	Siltstone	132	33	646	28	121	26	35	87	9.17	10.15	20.56	2.33
JNZ 32	Dolostone	394	26	1937	35	107	44	22	64	7.44	6.28	14.55	1.73
JNZ 33	Siltstone	323	54	5	26	82	33	57	167	12.84	12.03	26.74	3.25
JNZ 34	Dolostone	74	12	3264	27	84	14	50	57	4.35	3.73	9.29	1.09
JNZ 35	Siltstone	317	44	45,385	51	143	25	117	178	10.63	16.35	29.14	3.64
JNZ 36	Dolostone	145	6	1473	25	96	23	9	29	6.84	3.34	8.49	1.13
JNZ 37	Siltstone	373	47	36,282	41	96	23	92	256	3.37	4.14	11.05	1.34
JNZ 38	Dolostone	3602	13	229	27	223	9	44	58	11.28	8.44	27.66	2.16
JNZ 39	Dolostone	124	6	1325	25	91	14	43	62	9.94	7.48	17.18	2.08
JNZ 40	Siltstone	214	32	34,753	34	131	18	89	113	12.65	16.74	33.65	3.82
JNZ 41	Dolostone	144	6	943	27	106	12	33	33	13.26	7.45	19.96	2.38
JNZ 42	Breccia	244	17	52	46	54	12	78	172	25.38	21.24	46.56	5.57
JNZ 43	Siltstone	265	26	63	27	32	5	219	84	4.14	3.36	7.76	1.08
JNZ 44	Siltstone	342	26	517	38	51	13	120	95	13.65	12.35	31.85	3.76
JNZ 45	Siltstone	331	38	1727	48	123	12	76	159	12.36	16.42	31.98	3.73
JNZ 46	Breccia	230	23	1624	30	113	11	102	339	7.37	9.06	19.03	2.14
JNZ 47	Dolostone	132	15	686	44	106	12	85	212	6.75	4.97	11.53	1.45
JNZ 48	Dolostone	53	16	127	33	124	13	73	126	6.24	5.84	13.13	1.56

**Continued**

JNZ 49	Dolostone	56	13	103	30	145	12	51	37	4.24	4.42	9.53	1.25
JNZ 50	Dolostone	71	11	64	34	123	16	56	39	6.75	6.43	14.42	1.68
JNZ 51	Dolostone	57	13	58	25	72	25	78	49	5.66	4.93	13.65	1.47
JNZ 52	Siltstone	778	31	124	47	78	17	98	83	3.97	4.65	11.94	1.68
JNZ 53	Siltstone	944	34	625	63	164	15	36	67	7.84	11.46	23.86	2.57
JNZ 54	Siltstone	1163	60	48,458	90	264	43	28	88	11.16	12.68	34.27	3.82
JNZ 55	Dolostone	5601	12	2202	37	263	14	2	23	6.45	4.47	10.01	1.26
JNZ 56	Breccia	4773	37	216	56	262	15	38	105	14.52	15	27.05	3.25
JNZ 57	Dolostone	423	23	9401	31	133	25	26	46	9.04	6.04	13.62	1.74
JNZ 58	Dolostone	62	8	6138	25	144	12	7	33	6.17	3.46	8.98	1.17
JNZ 59	Dolostone	42	6	932	34	165	11	35	58	6.27	4.07	11.7	1.25
JNZ 60	Dolostone	76	83	56	33	94	21	18	51	5.96	5.08	13.47	1.47
JNZ 61	Dolostone	76	376	54	38	77	12	19	62	6.46	3.99	9.72	1.18
JNZ 62	Dolostone	193	34	4526	50	124	19	42	146	8.87	8.69	18.49	2.06
JNZ 63	Dolostone	76	9	84	40	98	19	30	57	5.02	5.12	11.25	1.37
JNZ 64	Dolostone	11	6	35	41	53	21	27	49	1.26	1.23	3.18	0.36
JNZ 65	Siltstone	196	24	51	51	196	23	38	58	1.24	2.14	4.46	0.55
JNZ 66	Dolostone	54	11	33	43	122	16	34	72	2.02	2.24	5.16	0.54
JNZ 67	Dolostone	52	7	22	40	123	15	25	32	4.42	4.32	44.15	1.13
JNZ 68	Dolostone	273	14	946	47	145	23	37	93	8.47	8.08	16.78	2.15
JNZ 69	Dolostone	305	15	1182	45	138	26	5	46	7.84	8.66	18.36	2.24
JNZ 70	Dolostone	323	32	11,055	67	141	30	35	107	13.66	14.33	28.45	3.43
JNZ 71	Dolostone	57	7	2052	29	101	17	21	59	6.8	7.38	16.63	1.96
JNZ 72	Siltstone	597	41	16,395	61	138	35	43	134	13.51	15.59	32.48	4.04
JNZ 73	Dolostone	206	8	7748	34	144	23	2	41	5.55	7.06	14.88	1.83
JNZ 74	Siltstone	192	8	5185	62	185	24	12	75	8.73	10.18	20.23	2.55
JNZ 75	Siltstone	2749	42	44,708	67	176	37	45	163	14.54	13.53	26.52	3.34
JNZ 76	Dolostone	473	8	4196	37	108	31	2	64	3.7	6.04	12.43	1.55
JNZ 77	Siltstone	343	32	13,568	56	193	22	40	77	13.34	15.75	39.86	3.98
JNZ 78	Siltstone	274	31	2315	56	189	13	12	78	10.55	13.09	26.33	3.17
JNZ 79	Siltstone	318	55	20,941	43	107	25	13	82	14.05	14.76	31.35	3.99
JNZ 80	Dolostone	277	31	2197	87	147	27	2	86	12.6	13.43	27.42	3.28
JNZ 81	Siltstone	188	8	1314	45	177	16	2	53	7.76	7.64	16.49	2.05
JNZ 82	Siltstone	268	45	7	53	124	187	56	203	14.05	12.11	25.28	3.02
JNZ 83	Dolostone	148	173	195	47	115	18	30	67	9.14	7.66	48.95	1.73
JNZ 84	Dolostone	224	17	98	46	123	16	18	82	9.23	5.65	13.64	1.41
JNZ 85	Dolostone	487	67	9677	40	83	23	17	76	5.94	6.58	13.25	1.52

**Continued**

JNZ 86	Siltstone	324	568	9340	42	192	14	2	57	8.85	9.8	21.86	2.41
JNZ 87	Dolostone	462	965	1459	44	172	12	36	267	10.64	7.69	16.98	1.84
JNZ 88	Dolostone	158	174	8687	30	145	17	56	244	7.94	5.98	13.53	1.62
JNZ 89	Siltstone	341	56	57,888	27	66	36	57	206	1.25	0.74	2.67	0.32
JNZ 90	Siltstone	186	22	5223	35	138	12	48	102	6.76	8.35	19.09	2.04
JNZ 91	Dolostone	156	113	7333	32	135	13	49	213	7.04	6.47	13.33	1.63
JNZ 92	Dolostone	782	523	2071	41	134	14	30	155	8.33	5.24	11.66	1.38
JNZ 93	Dolostone	293	100	783	27	123	10	24	94	5.83	7.13	36.85	1.66
JNZ 94	Dolostone	56	18	2315	39	145	14	16	105	6.03	4.06	9.34	1.16
JNZ 95	Dolostone	277	46	10,904	49	152	24	11	97	9.33	11.87	23.63	2.86
JNZ 96	Siltstone	74	30	284	25	112	10	54	267	6.24	4.74	10.93	1.37
JNZ 97	Dolostone	33	30	914	31	114	11	13	42	5.34	3.49	8.92	1.17
Sample	Rock type	Nd	Sm	Eu	Gd	Tb	Dy	Ho	Er	Tm	Yb	Lu	Th
JNZ 01	Siltstone	15.76	3.12	0.68	3.06	0.42	2.45	0.48	1.52	0.23	1.53	0.23	4.78
JNZ 02	Dolostone	10.44	2.283	0.62	2.72	0.37	2.008	0.35	0.95	0.11	0.72	0.1	1.08
JNZ 03	Dolostone	10.15	2.05	0.49	2.07	0.28	1.64	0.32	0.98	0.13	0.93	0.13	2.87
JNZ 04	Siltstone	13.26	2.582	0.58	2.47	0.33	1.92	0.38	1.19	0.16	1.17	0.17	3.85
JNZ 05	Dolostone	8.84	2.13	0.58	2.54	0.37	2.13	0.38	1.04	0.14	0.81	0.12	1.23
JNZ 06	Dolostone	11.94	2.44	0.59	2.39	0.33	2	0.43	1.23	0.17	1.18	0.17	3.46
JNZ 07	Siltstone	10.04	2.08	0.49	4	0.26	1.67	0.35	1.04	0.15	0.91	0.16	2.44
JNZ 08	Dolostone	14.83	3.48	0.99	4.2	0.63	3.58	0.63	1.65	0.19	1.182	0.16	1.34
JNZ 09	Siltstone	14.77	2.98	0.66	5	0.44	2.52	0.48	1.47	0.22	1.33	0.23	3.77
JNZ 10	Dolostone	10.52	2.38	0.64	2.63	0.43	2.32	0.45	1.17	0.16	0.94	0.14	1.54
JNZ 11	Dolostone	8.88	1.81	0.52	1.68	0.21	1.34	0.29	0.88	0.12	0.94	0.15	2.34
JNZ 12	Breccia	13.94	2.73	0.72	2.83	0.41	2.54	0.53	1.67	0.23	1.63	0.23	4.37
JNZ 13	Dolostone	7.33	1.95	0.66	2.65	0.36	1.95	0.35	0.98	0.14	0.76	0.12	1.16
JNZ 14	Dolostone	8.51	2.12	0.53	2.26	0.36	1.96	0.36	1.03	0.13	0.88	0.11	1.73
JNZ 15	Dolostone	9.32	1.92	0.56	2.13	0.34	1.86	0.37	1.33	0.17	1.07	0.16	1.76
JNZ 16	Siltstone	9.65	2.12	0.56	2.18	0.33	1.75	0.32	0.86	0.13	0.87	0.14	1.54
JNZ 17	Dolostone	6.42	1.33	0.35	1.28	0.12	0.94	0.16	0.48	0.08	0.47	0.08	0.73
JNZ 18	Dolostone	7.92	1.64	0.44	1.73	0.25	1.31	0.24	0.68	0.08	0.66	0.08	1.74
JNZ 19	Dolostone	6.43	1.58	0.53	1.76	0.26	1.42	0.25	0.67	0.08	0.58	0.08	0.73
JNZ 20	Siltstone	8.73	1.85	0.51	2.12	0.29	1.54	0.29	0.84	0.13	0.82	0.12	1.95
JNZ 21	Siltstone	12.32	2.46	0.62	2.5	0.35	2.08	0.43	1.34	0.23	1.47	0.22	4.15
JNZ 22	Dolostone	10.38	2.35	0.631	2.77	0.38	2.09	0.35	0.98	0.12	0.89	0.12	1.82
JNZ 23	Breccia	7.96	1.876	0.56	2.24	0.31	1.81	0.31	0.93	0.12	0.86	0.11	1.78
JNZ 24	Dolostone	11.18	2.57	0.6	2.78	0.42	2.51	0.47	1.32	0.16	1.14	0.15	1.77

**Continued**

JNZ 25	Dolostone	7.19	1.66	0.45	1.89	0.28	1.73	0.31	0.87	0.13	0.76	0.12	0.88
JNZ 26	Dolostone	18.42	3.923	1.04	4.23	0.45	3.35	0.61	1.73	0.22	1.44	0.2	2.71
JNZ 27	Dolostone	7.82	1.55	0.33	1.47	0.21	1.16	0.22	0.69	0.09	0.68	0.09	1.68
JNZ 28	Siltstone	9.38	2.133	0.54	2.4	0.26	2.003	0.34	0.92	0.11	0.7	0.09	0.53
JNZ 29	Dolostone	6.84	1.75	0.44	2.05	0.31	1.83	0.33	0.84	0.12	0.71	0.09	0.56
JNZ 30	Dolostone	10.54	2.43	0.65	2.84	0.4	2.34	0.44	1.23	0.15	1.02	0.13	1.74
JNZ 31	Siltstone	9.27	1.95	0.76	2.13	0.21	1.65	0.32	0.86	0.13	0.82	0.12	1.85
JNZ 32	Dolostone	7.05	1.66	0.55	1.86	0.26	1.46	0.25	0.7	0.09	0.63	0.08	1.07
JNZ 33	Siltstone	13.04	2.64	0.53	2.47	0.36	2.22	0.47	1.52	0.24	1.62	0.24	3.72
JNZ 34	Dolostone	4.48	1.04	0.33	1.22	0.17	0.72	0.16	0.38	0.07	0.31	0.04	0.44
JNZ 35	Siltstone	13.79	2.46	0.55	2.43	0.34	1.98	0.44	1.46	0.23	1.58	0.25	5.93
JNZ 36	Dolostone	5.91	1.44	0.4	1.74	0.27	1.43	0.25	0.58	0.08	0.46	0.07	0.17
JNZ 37	Siltstone	5.06	1.04	0.33	0.98	0.15	0.91	0.23	0.75	0.13	0.92	0.15	1.95
JNZ 38	Dolostone	8.97	2.23	1.56	2.85	0.37	2.07	0.36	1.06	0.15	0.91	0.16	1.47
JNZ 39	Dolostone	8.82	2.25	0.61	2.49	0.36	1.98	0.36	0.96	0.13	0.78	0.12	0.66
JNZ 40	Siltstone	14.73	2.87	0.61	2.88	0.38	2.29	0.46	1.45	0.22	1.44	0.22	5.12
JNZ 41	Dolostone	10.35	2.68	0.79	3.14	0.46	2.42	0.43	1.14	0.14	0.84	0.13	0.71
JNZ 42	Breccia	22.53	4.55	1.057	4.69	0.68	4.2	0.87	2.77	0.39	2.69	0.39	4.43
JNZ 43	Siltstone	4.03	0.87	0.29	0.92	0.14	0.93	0.2	0.56	0.09	0.57	0.07	1.21
JNZ 44	Siltstone	14.85	3.05	0.73	3.06	0.4	2.57	0.53	1.57	0.25	1.53	0.25	4.22
JNZ 45	Siltstone	13.79	2.62	0.52	2.57	0.36	2.09	0.44	1.37	0.22	1.33	0.21	4.81
JNZ 46	Breccia	8.11	1.63	0.44	1.67	0.25	1.36	0.29	0.87	0.11	0.85	0.12	1.77
JNZ 47	Dolostone	5.83	1.38	0.35	1.46	0.23	1.19	0.23	0.64	0.04	0.53	0.09	0.74
JNZ 48	Dolostone	6.14	1.37	0.36	1.42	0.21	1.09	0.23	0.57	0.06	0.45	0.04	1.02
JNZ 49	Dolostone	4.93	1.13	0.22	1.14	0.17	0.78	0.13	0.38	0.04	0.31	0.06	0.46
JNZ 50	Dolostone	6.71	1.55	0.42	1.76	0.27	1.26	0.24	0.58	0.08	0.41	0.07	0.74
JNZ 51	Dolostone	5.94	1.32	0.35	1.44	0.16	0.95	0.16	0.48	0.07	0.32	0.05	0.28
JNZ 52	Siltstone	6.66	1.44	0.44	1.23	0.14	0.94	0.18	0.63	0.08	0.63	0.1	1.21
JNZ 53	Siltstone	9.68	1.59	0.56	1.89	0.25	1.42	0.29	0.87	0.12	0.85	0.16	2.83
JNZ 54	Siltstone	13.87	2.71	0.78	2.68	0.39	2.04	0.44	1.24	0.16	1.17	0.15	4.52
JNZ 55	Dolostone	5.24	1.33	1.79	1.82	0.24	1.18	0.23	0.53	0.07	0.43	0.07	0.52
JNZ 56	Breccia	12.57	2.58	1.93	3.17	0.46	2.57	0.55	1.57	0.23	1.47	0.26	3.27
JNZ 57	Dolostone	6.97	1.55	0.49	2.02	0.34	1.63	0.34	0.82	0.11	0.66	0.08	1.33
JNZ 58	Dolostone	5.03	1.33	0.35	1.46	0.2	1.12	0.22	0.53	0.07	0.36	0.06	0.33
JNZ 59	Dolostone	5.35	1.35	0.36	1.52	0.21	1.14	0.23	0.53	0.06	0.36	0.06	0.36
JNZ 60	Dolostone	6.62	1.48	0.34	1.58	0.21	1.06	0.15	0.54	0.08	0.46	0.05	0.86
JNZ 61	Dolostone	5.53	1.37	0.33	1.48	0.18	1.07	0.17	0.53	0.07	0.44	0.07	0.66

**Continued**

JNZ 62	Dolostone	8.85	1.97	0.45	2.17	0.29	1.57	0.27	0.83	0.12	0.72	0.13	1.62
JNZ 63	Dolostone	5.26	1.06	0.24	1.05	0.15	0.73	0.13	0.38	0.06	0.37	0.05	0.63
JNZ 64	Dolostone	1.44	0.26	0.09	0.29	0.03	0.24	0.05	0.13	0.03	0.12	0.03	0.18
JNZ 65	Siltstone	1.95	0.33	0.13	0.3	0.03	0.23	0.05	0.13	0.03	0.15	0.04	0.44
JNZ 66	Dolostone	2.13	0.42	0.12	0.43	0.05	0.34	0.06	0.22	0.04	0.22	0.03	0.25
JNZ 67	Dolostone	4.27	0.89	0.22	1.15	0.14	0.68	0.14	0.36	0.06	0.34	0.04	0.43
JNZ 68	Dolostone	8.47	1.88	0.52	1.96	0.28	1.68	0.32	0.88	0.14	0.86	0.14	1.45
JNZ 69	Dolostone	8.95	1.99	0.54	2.06	0.32	1.68	0.32	0.88	0.13	0.85	0.13	1.53
JNZ 70	Dolostone	13.25	2.72	0.65	2.85	0.42	2.41	0.47	1.54	0.23	1.53	0.24	3.88
JNZ 71	Dolostone	7.82	1.64	0.418	1.71	0.23	1.29	0.23	0.64	0.08	0.56	0.08	0.87
JNZ 72	Siltstone	15.55	3.43	0.84	3.25	0.45	2.62	0.52	1.62	0.24	1.62	0.25	3.85
JNZ 73	Dolostone	7.12	1.46	0.42	1.58	0.22	1.07	0.18	0.52	0.06	0.41	0.05	0.94
JNZ 74	Siltstone	9.72	1.93	0.94	2.08	0.26	1.65	0.33	1.02	0.16	1.04	0.15	2.86
JNZ 75	Siltstone	12.79	2.597	0.95	2.62	0.38	2.57	0.57	1.92	0.29	2.07	0.3	4.66
JNZ 76	Dolostone	5.92	1.17	0.37	1.18	0.14	0.75	0.13	0.37	0.04	0.32	0.04	0.33
JNZ 77	Siltstone	15.47	3.104	0.75	3.15	0.43	2.48	0.47	1.44	0.2	1.37	0.19	3.65
JNZ 78	Siltstone	12.12	2.35	0.56	2.36	0.34	1.91	0.38	1.22	0.17	1.22	0.17	3.02
JNZ 79	Siltstone	15.53	3.14	0.74	3.07	0.43	2.62	0.53	1.72	0.25	1.76	0.25	4.24
JNZ 80	Dolostone	12.76	2.55	0.55	2.54	0.35	2.15	0.44	1.33	0.23	1.37	0.22	3.36
JNZ 81	Siltstone	8.15	1.82	0.48	3	0.27	1.54	0.26	0.71	0.09	0.58	0.08	0.86
JNZ 82	Siltstone	12.13	2.52	0.58	2.56	0.39	2.45	0.53	1.52	0.24	1.62	0.24	3
JNZ 83	Dolostone	8.13	1.87	0.45	2.36	0.27	1.58	0.25	0.78	0.1	0.67	0.08	1.17
JNZ 84	Dolostone	7.02	1.84	0.47	2.13	0.27	1.65	0.26	0.77	0.08	0.59	0.06	0.58
JNZ 85	Dolostone	7.04	1.45	0.37	1.52	0.19	1.07	0.25	0.63	0.09	0.62	0.07	1.92
JNZ 86	Siltstone	9.95	2.16	0.52	2.34	0.28	1.65	0.24	0.83	0.12	0.76	0.13	1.82
JNZ 87	Dolostone	8.26	1.94	0.53	2.24	0.32	1.85	0.33	0.98	0.14	0.89	0.11	0.82
JNZ 88	Dolostone	7.34	1.78	0.444	1.91	0.25	1.47	0.26	0.72	0.09	0.61	0.09	0.77
JNZ 89	Siltstone	1.27	0.32	0.14	0.34	0.06	0.38	0.05	0.29	0.05	0.35	0.06	0.87
JNZ 90	Siltstone	8.65	1.82	0.43	1.87	0.26	1.26	0.26	0.63	0.1	0.57	0.09	1.37
JNZ 91	Dolostone	7.24	1.64	0.48	1.77	0.24	1.24	0.24	0.63	0.08	0.56	0.08	0.96
JNZ 92	Dolostone	6.46	1.72	0.55	2.03	0.29	1.56	0.27	0.72	0.09	0.63	0.09	0.46
JNZ 93	Dolostone	7.13	1.45	0.34	1.65	0.18	1.07	0.22	0.67	0.1	0.68	0.11	1.86
JNZ 94	Dolostone	5.45	1.376	0.35	1.54	0.19	1.15	0.18	0.55	0.07	0.48	0.08	0.48
JNZ 95	Dolostone	12.19	2.29	0.48	2.33	0.24	1.53	0.32	0.96	0.13	0.96	0.13	3.09
JNZ 96	Siltstone	6.23	1.47	0.31	1.54	0.19	1.12	0.23	0.56	0.07	0.48	0.07	0.98
JNZ 97	Dolostone	5.45	1.45	0.32	1.54	0.19	1.04	0.16	0.46	0.04	0.33	0.06	0.29

## 6. Discussion

In the Jbel N'Zourk copper deposit, the mineralization is present at a macroscopic scale as a stockwork, disseminations and in karst pockets. The stockwork is composed by veins and veinlets filled with two successive mineralization phases:

- 1) A primary paragenesis composed by: bornite, chalcopyrite, associated with dolomite, quartz and calcite;
- 2) A secondary paragenesis composed by: covellite, chalcocite, digenite, malachite, azurite, chrysocolla, tenorite and cuprite associated with a gangue composed mainly of quartz-dolomite.

The veins and veinlets of this stockwork are oblique to the stratification plane. The majority of fractures families always present the same paragenetic evolution, mineralogy and textural. In consequence these different observations suggest that, with respect to the primary paragenesis of sulphides, all stockwork veins and veinlets are co-genetic (formed during in the same mineralization event). Microscopic studies reveal that the disseminations mineralizations correspond to microcracks and micro-fractures filled with the same mineralogical content, and texture characteristics as stockwork veins. In addition, disseminated copper containing mineral grains are directly connected to the stockwork veins. Consequently, all primary mineralization, from macroscopic to microscopic scale, is connected to the stockwork and deposited during a same hydrothermal fluid-assisted fracturing event of the host sedimentary rocks. Currently, according to the All these observations favor an epigenetic origin of the Jbel N'Zourk copper mineralization. In addition, the principal component analysis (PCA) of chemical data shows that copper does not have affinities with any of the lithological groups (siltstone, dolostone and breccias) present in the area. This result is also consistent with an epigenetic origin of the mineralization.

In comparison with most of the copper occurrences hosted in the Adoudouanian cover of the Central Anti-Atlas, the Jbel N'Zourk deposit shows a particularity that is reflected in the association of mineralization with tectonic structures, this is confirmed by structural, microstructural and metallographic study. Both families of fractures NNW-SSE and E-W, also the folds associated with the main fault of Jbel N'Zourk, served as a main drain that controlled the placement of the mineralization. Many authors evoke a Variscan remobilization of a primary syngenetic mineralization within the Adoudou formation to explain the stockwork textures intersecting sedimentary structures [1] [4] [9].

[1] describes kink bands and a rough cleavage developed in the vicinity of the previous fractures along the borders of the Bou Azzer El Graara inlier in the late Palaeozoic compressional event, generating in meter to decameter detachment folds scale which are common in the Adoudou formation, having a dominant NW-SE trending axes with subordinate NE-SW structures [1] [17]. These authors interpret these folds in terms of reactivation of Panafrican structures of the basement during the variscan orogenesis. In the Jbel N'Zourk the folds are associated locally with kilometre-scale sinistral strike-slip faults and SW-verging

transpressional reverse faults, where the Adoudou formation coming, via an inverse play, on the unit of siltstones and sandstones of the series of "Lie de Vin". This fault probably served as principal drain for the hydrothermal fluids that formed the mineralization of the Jbel N'Zourk deposit. Under such conditions, the age of the copper mineralization event at the Jbel N'Zourk deposit could probably be contemporary to the deformation of the cover during late Paleozoic compression. Currently, we propose that the copper mineralization presented in the Adoudou formation of the late Ediacaran to lower Cambrian cover is related to the variscan reactivation of the basement structures and addition to the variscan faults that drained the hydrothermal fluids which precipitated its copper content as a stockwork in the deformed terrains of the Jbel N'Zourk.

## 7. Conclusions

The copper mineralization in the Jbel N'Zourk deposit is epigenetic and is controlled by variscan tectonic structures that are associated with folding in the Adoudou formation. As a consequence, the copper mineralizing event occurred during this period. Most of the copper mineralization is present as stockwork, in fractures, faults and karst fill pockets. The location of the better-mineralized zone near faults and fractures indicates that it was epigenetic mineralization; it is possible that it occurred during the late variscan shortening. The position of the Jbel Boho volcanic series just below the mineralization can explain the origin of hydrothermal fluids.

The benefits of such an approach have a dual interest; 1) Scientific, contributes to a better understanding of the mechanism of vein formation process and understanding of the relationship between copper deformation-mineralization in the Adoudounian cover of the Central Anti Atlas, and 2) economics, contributes to a better knowledge of specific ore body geometry and distribution, thus the deformation affected the terrain and hence highly recommended in exploration program, but can also provide solutions to the exploitation problems.

## Acknowledgements

The authors would like to thank all those who have contributed, directly or indirectly, to its elaboration, to who have been teaching, guiding and encouraging. The thanks are also addressed to the MANAGEM group (SOMIFER) for their collaboration and help during the field survey, as well as the reviewers for their helpful comments and suggestions.

## Conflicts of Interest

The authors declare no conflicts of interest regarding the publication of this paper.

## References

- [1] Soulaimani, A. and Burkhard, M. (2008) The Anti-Atlas Chain (Morocco): The

Southern Margin of the Variscan Belt along the Edge of the West African Craton. *Geological Society of London*, **297**, 433-452. <https://doi.org/10.1144/SP297.20>

- [2] Bouchta, R., Boyer, F., Routhier, P., Saadi, M. and Salem, M. (1977) L'aire cuprifère de l'Anti-Atlas (Maroc); Permanence et arêtes riches. *Centre de Recherche Académique Scientifique*, **284**, 503-506.
- [3] Skacel, J. (1993) Gisement cuprifère polygénétique de Tazalaght (Anti-Atlas occidental). *Mine, Géologie et Energie*, **54**, 127-133.
- [4] Bensaou, M. and Hamoumi, N. (1999) Paléoenvironments et minéralisations de l'Anti-Atlas occidental marocain au Cambrien précoce. *Chronique de la recherche minière*, **536-537**, 113-119.
- [5] Maacha, L., Ennaciri, O., El Ghorfi, M., Baoutoul, H., Saquaque, A. and Soulaimani, A. (2011) The Jbel La'sal oxidized copper deposit (El Graara inlier, central Anti-Atlas). Les principales mines du Maroc. *Notes et Mémoires de Service Géologique du Maroc*, **564**, 117-121.
- [6] Madi, O., Baoutoul, H., Maacha, L., Ennaciri, O. and Soulaimani, A. (2011) La mine d'Agjal au sud du Kerdous ; considérations sur les gîtes stratoïdes de cuivre et argent de l'Anti-Atlas occidental et central. *Nouveaux Guides Géologiques Et Miniers Du Maroc*, **9**, 151-156.
- [7] Maacha, L., Ennaciri, O., Saquaque, A. and Soulaimani, A. (2017) A Promizing Prospect: The Jbel N'Zourk Deposit (Central Anti-Atlas). Les Principales Mines du Maroc. *Notes et Mémoires de Service Géologique du Maroc*, **564**, 123-127.
- [8] Service Géologique du Maroc (1985) Carte géologique du Maroc au 1/1000000. Notes et Mémoires du Service Géologique du Maroc 260.
- [9] Soulaimani, A., Michard, A. and Ouanaimi, H. (2014) Late Ediacaran-Cambrian Structures and Their Reactivation during the Variscan and Alpine Cycles in the Anti-Atlas (Morocco). *Journal of African Earth Sciences*, **98**, 94-112. <https://doi.org/10.1016/j.jafrearsci.2014.04.025>
- [10] Ennih, N. and Liegeois, J.P. (2001) The Moroccan Anti-Atlas: The West African Craton Passive Margin with Limited Pan-African Activity. Implications for the Northern Limit of the Craton. *Precambrian Research*, **112**, 289-302. [https://doi.org/10.1016/S0301-9268\(01\)00195-4](https://doi.org/10.1016/S0301-9268(01)00195-4)
- [11] Malek, H.A., Gasquet, D., Bertrand, J.M. and Leterrier, J. (1998) Géochronologie U-Pb sur zircon de granitoïdes éburnéens et panafricains dans les boutonnières protérozoïques d'Igherm, du Kerdous et du Bas Drâa (Anti-Atlas occidental, Maroc). *Comptes Rendus de l'Académie des Sciences—Series IIA—Earth and Planetary Science*, **327**, 819-826. [https://doi.org/10.1016/S1251-8050\(99\)80056-1](https://doi.org/10.1016/S1251-8050(99)80056-1)
- [12] Choubert, G. (1947) L'accident majeur de l'Anti-Atlas. *Comptes Rendus de l'Académie des Sciences Paris*, **224**, 1172-1173.
- [13] Leblanc, M. (1975) Ophiolites précambriniennes et gîtes arsénés de cobalt (Bou-Azzer, Maroc). Master's Thesis, Université de Paris VI, Paris.
- [14] Saquaque, A., Admou, H., Cisse, A., Benyoussef, A. and Reuber, I. (1989) Les intrusions calco-alcalines de la boutonnière de Bou-Azzer-El Graara (Anti-Atlas): Marqueurs de la déformation panafricaine majeure dans un contexte de collision d'arc. *Comptes Rendus de l'Académie des Sciences Paris*, **308**, 1279-1283.
- [15] Leblanc, M. and Moussine-Pouchkine, A. (1994) Sedimentary and Volcanic Evolution of a Neoproterozoic Continental Margin (Bleïda, Anti-Atlas, Morocco). *Precambrian Research*, **70**, 25-44. [https://doi.org/10.1016/0301-9268\(94\)90019-1](https://doi.org/10.1016/0301-9268(94)90019-1)
- [16] Hefferan, K.P., Admou, H., Karson, J.A. and Saquaque, A. (2000) Anti-Atlas (Morocco) Role in Neoproterozoic Western Gondwana Reconstruction. *Precambrian*

*Research*, **103**, 89-96. [https://doi.org/10.1016/S0301-9268\(00\)00078-4](https://doi.org/10.1016/S0301-9268(00)00078-4)

- [17] Thomas, R.J., Chevallier, L.P., Gresse, P.G., Harmer, R.E., Eglington, B.M., Armstrong, R.A., de Beer, C.H., Martini, J.E.J., de Kock, G.S., Macey, P.H. and Ingram, B.A. (2002) Precambrian Evolution of the Sirwa Window, Anti-Atlas Orogen, Morocco. *Precambrian Research*, **118**, 1-57.  
[https://doi.org/10.1016/S0301-9268\(02\)00075-X](https://doi.org/10.1016/S0301-9268(02)00075-X)
- [18] Inglis, J.D., MacLean, J.S., Samson, S.D., D'Lemos, R.S., Admou, H. and Hefferan, K. (2004) A Precise U-Pb Zircon Age for the Bleïda Granodiorite, Anti-Atlas, Morocco: Implications for the Timing of Deformation and Terrane Assembly in the Eastern Anti-Atlas. *Journal of African Earth Sciences*, **39**, 277-283.  
<https://doi.org/10.1016/j.jafrearsci.2004.07.041>
- [19] D'Lemos, R.S., Inglis, J.D. and Samson, S.D. (2006) A Newly Discovered Orogenic Event in Morocco: Neoproterozoic Ages for Supposed Eburnean Basement of the Bou Azzer Inlier, Anti-Atlas Mountains. *Precambrian Research*, **147**, 65-78.  
<https://doi.org/10.1016/j.precamres.2006.02.003>
- [20] Soulaimani, A., Jaffal, M., Maacha, L., Kchikach, A., Najine, A. and Saidi, A. (2006) Modélisation magnétique de la suture ophiolitique de Bou Azzer-El Graara (Anti-Atlas central, Maroc). Implications sur la reconstitution géodynamique panafricaine. *Comptes Rendus Géosciences*, **338**, 153-160.  
<https://doi.org/10.1016/j.crte.2005.10.001>
- [21] Walsh, G.J., Benziiane, F., Aleinikoff, J.N., Harrison, R.W., Yazidi, A., Burton, W.C., Quick, J.E. and Saadane, A. (2012) Neoproterozoic Tectonic Evolution of the Jebel Saghro and Bou Azzer—El Graara Inliers, Eastern and Central Anti-Atlas, Morocco. *Precambrian Research*, **216-219**, 23-62.  
<https://doi.org/10.1016/j.precamres.2012.06.010>
- [22] Gasquet, D., Levresse, G., Cheilertz, A., Azizi-samir, M.R. and Mouttaqi, A. (2005) Contribution to a Geodynamic Reconstruction of the Anti-Atlas (Morocco) during Pan-African Times with the Emphasis on Inversion Tectonics and Metallogenetic Activity at the Precambrian—Cambrian Transition. *Precambrian Research*, **140**, 157-182.  
<https://doi.org/10.1016/j.precamres.2005.06.009>
- [23] Choubert, G. (1957) L'Adoudounien et le Précambrien III dans l'Anti-Atlas, et Les relations entre le Précambrien et le Cambrien. Centre National de la Recherche Scientifique, Paris.
- [24] Choubert, G. (1952) Histoire géologique du domaine de l'Anti-Atlas. *Notes et Mémoires de Service Géologique du Maroc*, **100**, 75-193.
- [25] Helg, U., Burkhard, M., Carigt, S. and Robert-Charrue, C. (2004) Folding and Inversion Tectonics in the Anti-Atlas of Morocco. *Tectonics*, **23**, TC4006.  
<https://doi.org/10.1029/2003TC001576>
- [26] Belfoul, M.A. (2005) Cinématique de la déformation hercynienne et géodynamique C.W.A Paléozoïque dans l'Anti-atlas sud-occidental, et le Sahara Marocain. Master's Thesis, Université Ibn Zohr, Agadir.
- [27] Bensaou, M. and Hamoumi, N. (2003) Le graben de l'Anti-Atlas occidental (Maroc): Contrôle tectonique de la paléogéographie et des séquences au Cambrien inférieur. *Comptes Rendus Geoscience*, **335**, 297-305.  
[https://doi.org/10.1016/S1631-0713\(03\)00033-6](https://doi.org/10.1016/S1631-0713(03)00033-6)
- [28] Thomas, R.J., Fekkak, A., Ennih, N., Errami, E., Loughlin, S.C., Gresse, P.G., Chevallier, L.P. and Liegeois, J.P. (2004) A New Lithostratigraphic Framework for the Anti-Atlas Orogen, Morocco. *Journal of African Earth Sciences*, **39**, 217-226.  
<https://doi.org/10.1016/j.jafrearsci.2004.07.046>

- [29] Chevremont, P., Razin, P., Baudin, T., Gabudianu, D. Roger, J., Thieblemont, D., Calves, G. and Anzar, C. (2006) Mémoire explicatif, carte géologique du Maroc (1/500000), feuille Awkarda. *Notes et Mémoires de service géologique du Maroc*, **497**, 113-114.
- [30] Boudda, A., Choubert, G. and Faure-muret, A. (1979) Essai de stratigraphie de la couverture sédimentaire de l'Anti-Atlas: Adoudounien-Cambrien inférieur. Editions du Service géologique du Maroc, Rabat.
- [31] Geyer, G. (1990) Proposal of Formal Lithostratigraphical Units for the Terminal Proterozoic to Early Middle Cambrian of Southern Morocco. *Newsletters on Stratigraphy*, **22**, 87-109. <https://doi.org/10.1127/nos/22/1990/87>
- [32] Bensaou, M. and Hamoumi, N. (2004) Les Microbialites de L'Anti-Atlas Occidental (Maroc): Marqueurs Stratigraphiques et témoins des changements environnementaux au Cambrien inférieur. *Comptes Rendus Geoscience*, **336**, 109-116. <https://doi.org/10.1016/j.crte.2003.10.024>
- [33] Alvaro, J.J., Clausen, S., El Albani, A. and Chellai, E.H. (2005) Facies Distribution of Lower Cambrian Cryptic Microbial and Epibenthic Archaeocyathan-Microbial Communities in the Western Anti-Atlas, Morocco. *Sedimentology*, **53**, 35-53. <https://doi.org/10.1111/j.1365-3091.2005.00752.x>
- [34] Ducrot, J. and Lancelot, J.R. (1977) Problème de la limite Précambrien-Cambrien: Étude radiochronologique par la méthode U/Pb sur zircon du volcan du Jbel Boho. *Canadian Journal Earth Sciences*, **14**, 1771-1777. <https://doi.org/10.1139/e77-243>
- [35] Alvaro, J.J., Ezzouhairi, H., Vennin, E., Ribeiro, M.L., Clausen, S., Charif, A., Ait Ayad, N. and Moreira, M.E. (2006) The Early-Cambrian Boho Volcano of the El Graara Massif, Morocco: Petrology, Geodynamic Setting and Coeval Sedimentation. *Journal of African Earth Sciences*, **44**, 396-410. <https://doi.org/10.1016/j.jafrearsci.2005.12.008>